



Contents lists available at ScienceDirect

Journal of Hand Surgery Global Online

journal homepage: www.JHSGO.org

Original Research

Ulnar Bowing and Distal Radioulnar Joint Anatomy: A Three-Dimensional, *In Situ* Clinical Assessment



Samuel L. Shuman, BA, * Rade R. Jibawi Rivera, BS, * Farhan Ahmad, MD, *
Alejandro A. Espinoza Orías, PhD, * John F. Hoy, BA, * Xavier Simcock, MD *

* Rush University Medical Center, Chicago, IL

ARTICLE INFO

Article history:

Received for publication December 19, 2023

Accepted in revised form December 24, 2023

Available online February 19, 2024

Key words:

Distal radioulnar joint

Three-dimensional analysis

Ulnar bowing

Ulnar morphology

Ulnar variance

Purpose: Distal radioulnar joint (DRUJ) injuries can be devastating and challenging to manage. The multiplanar curvature exhibited by the ulna impacts the morphology of the DRUJ, making it difficult to assess through two-dimensional radiographs alone. We used full-length, three-dimensional (3D) computed tomography angiography scans to assess the relationship between ulnar bowing, DRUJ ulnar variance (UV), and sigmoid notch angle. The goal of this study was to establish normal anatomic ranges for these landmarks to improve treatment for forearm traumas and DRUJ pathologies.

Methods: Eighty-two intact upper extremity computed tomography angiography scans were examined and reconstructed into 3D models. We characterized ulnar bowing and DRUJ metrics using computer-aided design software. Measures of central tendency and Pearson correlation coefficients were calculated for comparative analysis.

Results: The study yielded an average ulnar length of 272.3 mm. We identified the proximal ulnar bow at 36.7% of the bone's total length, possessing a depth of 10.3 mm, a proximal angle of 6.6°, and a distal angle of 3.9°. The distal ulnar bow appeared at 75.3% of the bone's length, characterized by a depth of 4.2 mm, a proximal angle of 2°, and a distal angle of 4.3°. In the coronal plane, the proximal angle of the proximal ulnar bow correlated positively with UV ($r = 0.39, P < .001$), whereas the distal angle of the distal ulnar bow correlated negatively ($r = -0.48, P < .001$). We also found significant correlations between the depths of both proximal and distal bows with UV ($r = 0.38, P < .001$; $r = -0.34, P < .001$, respectively). Moreover, UV within the DRUJ strongly correlated with the sigmoid notch angle ($r = -0.77, P = .01$). In contrast, the sagittal plane metrics did not show meaningful correlations with UV.

Conclusion: Sagittal alignment and translation at the DRUJ articulation are directly related to ulna bowing at the distal ulna. A nuanced understanding of these 3D relationships can enhance preoperative planning when correcting ulnar-side pathology.

Type of study/level of evidence: Therapeutic IV.

Copyright © 2024, THE AUTHORS. Published by Elsevier Inc. on behalf of The American Society for Surgery of the Hand. This is an open access article under the CC BY-NC-ND license (<http://creativecommons.org/licenses/by-nc-nd/4.0/>).

The distal ulna and radius articulate at the distal radioulnar joint (DRUJ) of the forearm and play critical roles in wrist mechanics. At the DRUJ, various ligaments and joint capsule surfaces work with the ulna and radius to stabilize the joint to permit painless rotation and weight-bearing capacity of the forearm. Conditions and injury to the components of this intricate joint can be devastating to patients.^{1–4}

The distal ulna and ulnar-sided wrist pain, in general, has often been referred to as a “black box” of forearm pathology.⁵ This is partly due to the limited success of previous surgical interventions for wrist pain relief and relatively few research studies quantifying the morphology of the distal ulna's complex curvature and its relationship to the sigmoid notch of the radius at the DRUJ. However, recent surgical advances in this area have created newfound interest among the orthopedic community. Surgeons have lately had increased success with postoperative DRUJ outcomes; however, there remain anatomic knowledge gaps, particularly regarding the impact of ulnar bowing and its relation to DRUJ congruency.^{6–8}

Corresponding author: John Hoy, BA, Rush University Medical Center, Department of Orthopaedic Surgery, 1611 W. Harrison Street, Chicago, IL 60612.
E-mail address: john.hoy.research@gmail.com (J.F. Hoy).

<https://doi.org/10.1016/j.jhsg.2023.12.006>

2589-5141/Copyright © 2024, THE AUTHORS. Published by Elsevier Inc. on behalf of The American Society for Surgery of the Hand. This is an open access article under the CC BY-NC-ND license (<http://creativecommons.org/licenses/by-nc-nd/4.0/>).

The primary anatomical limit of these procedures is the morphology of the distal radial DRUJ. When the DRUJ is weakened or altered due to alterations of its bony and soft tissue structures, the patient often experiences wrist pain. This instability is typically a byproduct of various conditions and traumas, such as forearm fractures, ulnar impaction syndrome, and triangular fibrocartilage complex injury, which can each separately promote discomfort.^{1,9,10}

For corrective DRUJ procedures such as ulnar shortening osteotomy, the slightest of surgical modifications can have major consequences. Suboptimal ulnar resections or any minor deviations from the normal relationship of the ulna to the radius at the DRUJ can lead to articular mismatch, instability, inability to bear weight, and significant pain.^{1,11,12} Thus, during these procedures, the surgeon must be overcautious of any and all bone translations in the axial, sagittal, and coronal planes. Currently, wrist surgeons often shorten the ulna only in one or two planes of reference.^{12,13} With this incomplete information, they can be successful in shortening the longitudinal axis of the ulna, for example, but may subsequently promote joint mismatch or instability in other planes. The goal of this investigation was to analyze the morphology of the ulna and its relationship to the DRUJ in three dimensions. We hypothesize that significant clinical correlations exist between distal ulnar bowing and DRUJ anatomy and between sagittal ulnar bowing and DRUJ translation.

Materials and Methods

Population selection

Study approval was obtained by the Rush University Institutional Review Board before commencing the study. A total of 198 computed tomography angiography (CTA) scans of the upper extremity were performed at Rush University Medical Center between January 1, 2009, and December 31, 2020. Upper extremity CTAs were chosen because they are more likely to involve patients without any current or previous orthopedic pathology or trauma of the forearm. Scans were excluded in patients who had forearm fractures or implanted devices, if the image sets did not include 3 mm sets and if the region of interest did not show the distal end of the humerus and complete forearm. After applying these exclusion criteria, the remaining 82 arms were included in this study.

Software

We performed three-dimensional (3D) modeling and analysis using commercially available medical imaging segmentation and computer-aided design software. Mimics (Materialize Mimics v. 25 Research) was used to reconstruct the CTA Digital Imaging and Communications in Medicine data sets of all cases. The resulting 3D models were exported as .STL and .IGES files and analyzed using Rhinoceros v. 7.14 (Robert McNeel and Associates).

Segmentation

Upper extremity CTAs with 3-mm thick axial slices were imported separately into Mimics. An automatic threshold was first set to identify cortical bone based on Hounsfield units, creating a layer that only included the long bones of the arm and the bones of the hand. Any software-generated errors after threshold were corrected manually, and any defects in the cortical bone were filled in. The humerus, radius, and ulna for each subject were then isolated into their own layers. Finally, each bone was smoothed, reduced, and wrapped before being exported as .STL files for measurement and morphological analysis. For further analysis, centroid (center of mass) lines of both the segmented ulnae and radii were computed

in Mimics and subsequently exported as .IGES files. Of note, the filetypes themselves are not relevant, rather the 3D point cloud data and the relationships between points are important.

3D analysis

All of the segmented .STL and .IGES files were imported into Rhinoceros 3D to analyze ulnar bowing and the DRUJ in coronal, sagittal, and axial planes. To analyze ulnar bowing parameters, we used external radiographic landmarks based on a study by Hreha et al¹⁴ as reference points to measure bowing locations, magnitude, and angulation. All distances were recorded in millimeters. To analyze DRUJ parameters, we used distal ulnar and radial landmarks based on a study by Roner et al¹⁵ to measure ulnar variance (UV) and sigmoid notch angulation.

Ulnar bowing measurements

To measure ulnar bowing in the sagittal plane (Fig. 1), a coordinate plane was first aligned to bisect the epicondyles of the distal humerus to position the ulna. The coordinate plane was then slightly adjusted around its y-axis to obtain an accurate bisection of the ulna along its anterior–posterior plumb line; the ulnar centroid line was used for consistent creation of this coordinate plane across all subjects. To examine the sagittal bowing of the ulna, a reference line was drawn from the most dorsal and proximal end of the olecranon process to the most dorsal and distal end of the ulnar styloid. This line allowed for the identification of the external bow's most posterior or anterior point in the y-axis (point b), whose coordinates were recorded as the bow location in the sagittal plane. The length from the proximal end of the ulna to this point was normalized by dividing it by the length of the entire ulna, resulting in a percentage value. Bow depth was determined as the vertical distance between the reference line and point b. To measure the bowing angles, two additional lines were drawn connecting point b to either end of the reference line. The proximal bowing angle (a) was measured between the lines proximal to point b, and the distal bowing angle (c) was measured between the lines distal to point b.

To measure ulnar bowing in the coronal plane (Fig. 1), the aforementioned sagittal coordinate plane was rotated either 90° or 270° (depending on arm laterality) to align the ulna in the anteroposterior direction. The ulna has both a proximal and distal bow in the coronal plane as previously described by multiple authors.^{14,16,17} We used and modified a method described by Weber et al¹⁶ to examine coronal bowing. A reference line was drawn connecting the most medial point of the olecranon process to the most medial aspect of the ulnar head. This line allowed for the identification of the external bow's most ulnar point in the y-axis (point b), and point b was recorded as the bow location and converted to a percentage of the ulna's length. Two additional lines were drawn to connect the point b to the proximal and distal ends of the reference line. The proximal and distal angles of the proximal bow were measured between the lines proximal and distal to point b, respectively. The depth of the proximal bow was measured as the vertical distance between the reference line and point b. To measure the distal bow, we used and modified a method described by Hreha et al.¹⁴ A reference line was drawn connecting the most lateral aspect of the proximal end of the ulna to the most lateral aspect of the ulnar head. This line allowed for the identification of the external bow's most radial point in the y-axis (point e). Point e was recorded as the apex bow location and converted to a percentage of the ulna's length. Two additional lines were drawn to connect the point e to the proximal and distal ends of the reference line. The proximal and distal angles of the distal bow were measured between the lines proximal and distal to point e,

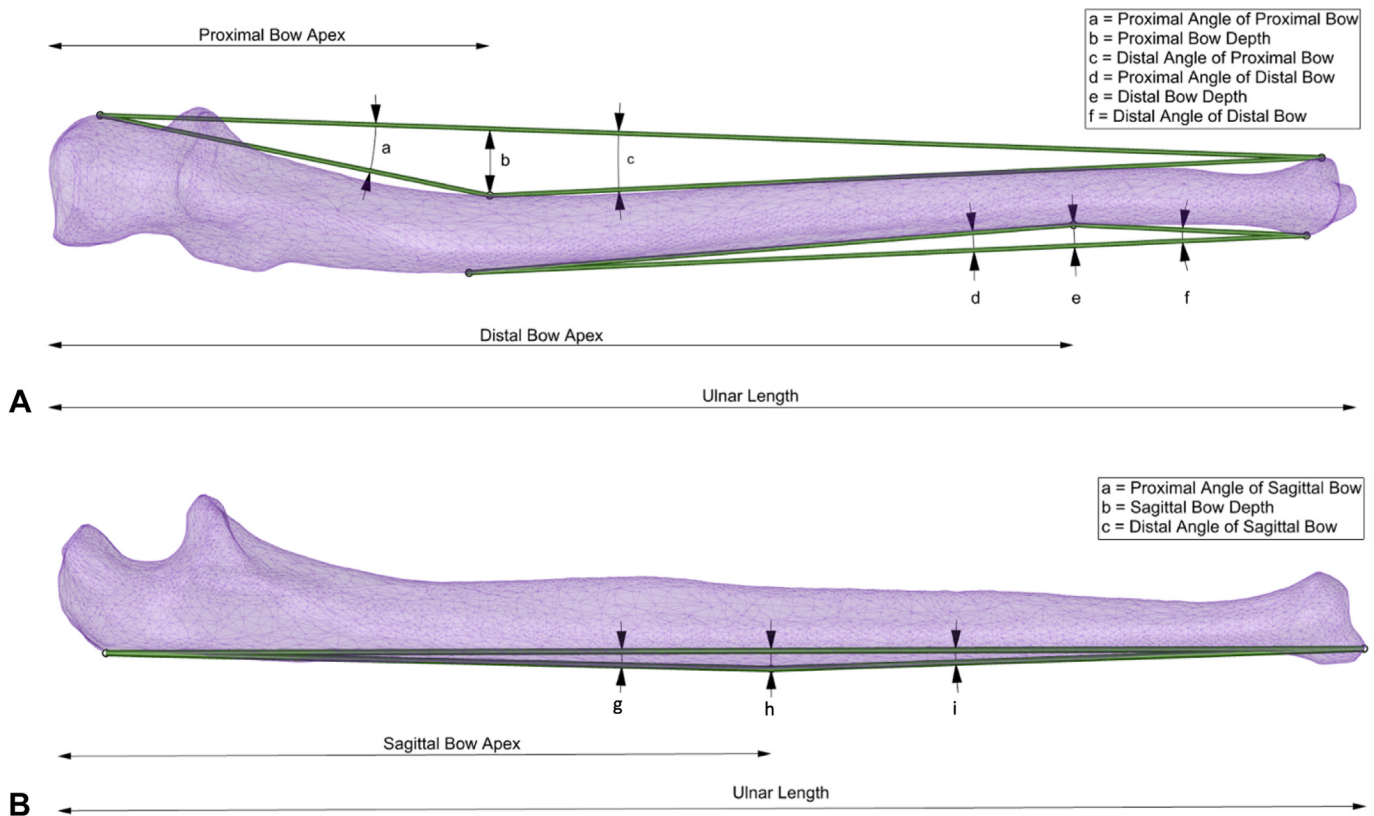


Figure 1. Measuring the ulnar bows. **A** Proximal ulnar bowing is measured by identifying the most ulnar aspects of the proximal and distal ulna. The bow apex, “b,” is identified as the furthest point on the ulna from the straight line connecting the most ulnar aspects. Distal ulnar bowing is measured by identifying the most radial aspects of the proximal and distal ulna. The bow apex, “e,” is identified as the furthest point on the ulna from the straight line connecting the most radial aspects. **B** Sagittal ulnar bowing is measured by identifying the most proximal, dorsal aspect at the level of the olecranon and drawing a straight line to the ulnar styloid. The bow apex, “h,” is identified as the furthest point on the dorsal ulna from the straight line.

respectively. The depth of the distal bow was measured as the vertical distance between the reference line and point b.

Measurement of DRUJ landmarks

The DRUJ was characterized using similar methodology as described by Roner et al.¹⁵ A coordinate plane was aligned to first set the axial view of the DRUJ. The origin was placed at the center of the distal radial face with the y-axis aligned to the dorsal tubercle, the x-axis aligned to the radial styloid, and the z-axis aligned to the anteroposterior plumb line. The DRUJ coronal plane was made from a 90° rotation around the x-axis followed by a 90° or 270° rotation around the z-axis of the axial plane (so that the x-axis would point proximally).

To measure the 3D UV, we identified the most distal point of the ulnar head and the center point of the distal sigmoid notch edge and measured the distance between them (Fig. 2). The distance was measured in the DRUJ coronal plane.

To measure the 3D sigmoid notch angle (SNA), we identified the most distal and proximal points of the sigmoid notch and modeled the contour of its face by placing multiple points in between. A best-fit line from these points was created. Using the axial plane, a best-fit arc tangent to the distal sigmoid notch ridge was fitted. The anteroposterior length of the sigmoid notch (via the best-fit line) and the radius of the arc were both measured. Next, we fit a circle to the arc and then extruded a cylinder to match the length of the sigmoid notch. A longitudinal axis of the cylinder was created. Finally, we identified and extruded the straightest portion of our radial centroid line at the metaphysis to serve as the longitudinal

axis of the segmented radius (Fig. 2). In the coronal plane, the angulation between lines x and y was measured to provide the SNA value.

Statistical analysis

Descriptive statistics were used to analyze ulnar and DRUJ morphology. Continuous variables are presented as means with standard deviations. Pearson’s correlation was used to assess for correlation between ulnar morphology, UV, and SNA.

Results

A total of $n = 74$ patients with $n_{CTA} = 82$ CTA imaged arms ($n_m = 39$ men and $n_f = 35$ women; 8 bilateral scans; 42 left arms, and 40 right arms) with a mean age of 50.5 years (range: 20–90 years old, SD = 16.96 years) were included in this study.

Sagittal plane measurements

The mean ulnar length was 272.3 ± 21.3 mm. The mean location of the sagittal ulnar bow was 140.8 ± 28.1 mm or $51.8 \pm 10.2\%$ of the entire length of the ulna. The mean sagittal bow depth was 3.4 ± 1.9 mm. The mean proximal angle was $2.0 \pm 1.3^\circ$, and the mean distal angle was $2.0 \pm 1.0^\circ$. Of the 82 ulnae, 6 were identified as concave-shaped (apex-anterior). The remaining were all convex-shaped (apex-posterior; Table 1).

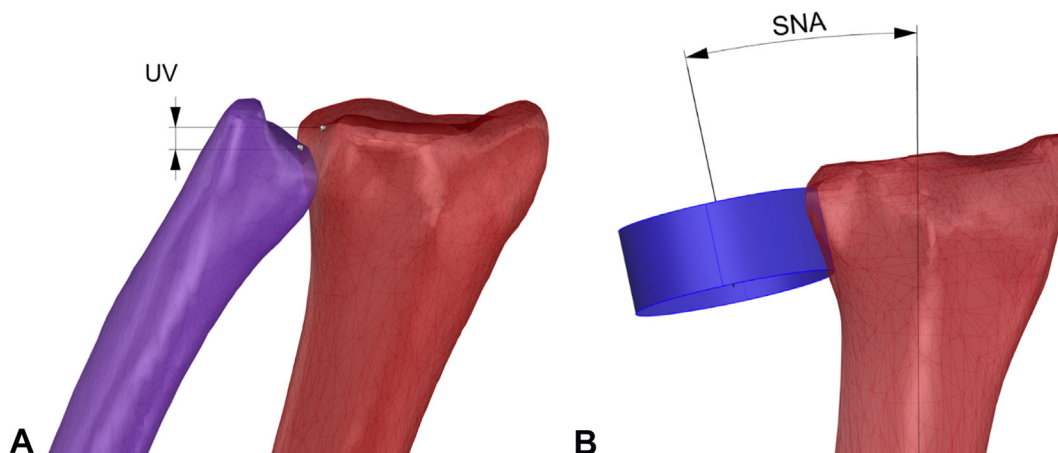


Figure 2. Measuring the distal radioulnar joint. **A** The ulnar variance is measured as the anteroposterior difference between the most distal point of the ulnar head (gray sphere on purple ulna) and the most radial point of the sigmoid notch edge (gray sphere on the red radius). **B** The sigmoid notch angle is measured as the angulation between the longitudinal axis of the radius (red bone) and the longitudinal axis of the “best fit” cylinder tangent to the sigmoid notch.

Table 1
Metrics of Coronal and Sagittal Ulnar Bowing (n = 82)

		Mean	95% CI	Range
Coronal: proximal bow	Ulna length, mm	272.3	267.7–276.9	228.4–323.5
	Bow location, %	36.7	36.0–37.3	72.4–123.5
	Bow apex, mm	99.7	97.4–102.0	28.5–43.5
	Bow depth, mm	10.3	9.7–10.9	5.7–17.1
	Proximal angle, °	6.6	6.3–6.9	4.0–9.9
Coronal: distal bow	Distal angle, °	3.9	3.8–4.1	2.6–5.5
	Bow location, %	75.3	74.30–76.27	65.0–91.0
	Bow apex, mm	204.8	200.8–208.9	166.9–264.5
	Bow depth, mm	4.2	3.9–4.6	0.9–8.8
	Proximal angle, °	2.0	1.82–2.12	0.4–3.4
Sagittal bow	Distal angle, °	4.3	4.0–4.7	0.8–7.9
	Bow location, %	51.77	49.7–53.9	19.6–69.6
	Bow apex, mm	140.8	134.8–146.9	44.9–189.9
	Bow depth, mm	3.4	3.0–3.8	0.1–8.6
	Proximal angle, °	2.0	1.7–2.3	0.03–7.7
	Distal angle, °	2.0	1.7–2.2	0.07–5.1

Coronal plane proximal and distal bow measurements

The mean location of the proximal coronal bow was 99.7 ± 10.4 mm or $36.7 \pm 3.2\%$ of the entire length of the ulna. The mean proximal bow depth was 10.3 ± 2.6 mm. The mean proximal angle was $6.6 \pm 1.4^\circ$, and the mean distal angle was $3.9 \pm 0.8^\circ$.

The mean location of the distal coronal bow was 204.9 ± 18.8 mm or $75.3 \pm 4.6\%$ of the entire length of the ulna. The mean proximal bow depth was 4.2 ± 1.7 mm. The mean proximal angle was $2.0 \pm 0.7^\circ$, and the mean distal angle was $4.3 \pm 1.6^\circ$.

In relation to angulation parameters, the proximal angle of the proximal ulnar bow correlated with the distal angle of the distal ulnar bow ($r = -0.31$, $P < .001$; Table 1).

DRUJ measurements

Ulnar variance measurements were stratified according to positive (≥ 1 mm), neutral ($-1 \geq x \geq -1$ mm), or negative (≤ -1 mm). The mean value in subjects with a positive UV (35/82) was 2.53 mm. The mean angulation in subjects with a neutral UV (31/82) was 0.3 mm. The mean angulation in subjects with a negative UV (16/82) was -2.0 mm.

Sigmoid notch angle measurements were also stratified according to positive ($\geq 1^\circ$), neutral ($-1 \geq x \geq -1^\circ$), or negative ($\leq -1^\circ$).

The mean angulation in subjects with a positive SNA (23/82) was 7° . The mean angulation in subjects with a neutral SNA (13/82) was 0.2° . The mean angulation in subjects with a negative SNA (46/82) was -6.7° . The mean sigmoid notch length, measured in the AP plane, was 9.5 mm. In relating the two parameters, UV positively correlated with the SNA ($r = -0.77$; Table 2).

Relating ulnar bowing to the DRUJ

When analyzed in the coronal plane, the proximal angle of the proximal ulnar bow correlated with UV ($r = 0.39$, $P < .001$), the distal angle of the distal ulnar bow correlated with UV ($r = -0.48$, $P < .001$), the depth of the proximal ulnar bow correlated with UV ($r = 0.38$, $P < .001$), and the depth of the distal ulnar bow correlated with UV ($r = -0.34$, $P < .001$). Distal angle bowing was also further analyzed by UV subgroups. In particular, subjects with a negative UV had a mean distal bowing angle of 5.2° and a moderate correlation between the two variables ($r = 0.48$, $P < .001$; Tables 3 and 4).

When analyzed in the sagittal plane, the sagittal bow depth, proximal angle, and distal angle all did not meaningfully correlate with UV ($r = -0.17$, -0.15 , and -0.18 , respectively, all $P < .001$; Table 3).

When analyzing the effect of distal bowing in the coronal plane on whether the ulnar head translates dorsally or volarly, we found

Table 2
Metrics of SNA and UV of the distal radioulnar joint (n = 82)*

	Mean	95% CI	Range
Positive SNA, ° (n _{SNP} = 23)	6.97	4.9–9.1	1–20.7
Neutral SNA, ° (n _{SNX} = 13)	0.24	–0.05 to 0.5	–0.9 to 0.9
Negative SNA, ° (n _{SNN} = 46)	–6.70	–8.1 to –5.3	–19.5 to –1.4
Sigmoid notch depth, mm	9.51	9.1–10.0	5.4–14.4
Positive UV, mm (n _{UVP} = 35)	2.53	2.1–2.9	1.1–5.0
Neutral UV, mm (n _{UVX} = 31)	0.28	–0.1 to 0.5	–0.7–1.0
Negative UV, mm (n _{UVN} = 16)	–2.00	–2.3 to –1.7	–3.4 to –1.1

* SNA measurements were categorized by positive SNA ($\geq 1^\circ$), neutral SNA ($1^\circ > x > -1^\circ$), or negative SNA ($\leq -1^\circ$). UV measurements were categorized by positive UV (≥ 1 mm), neutral UV ($1^\circ > x > -1$ mm), or negative UV (≤ -1 mm).

Table 3
Correlations Between Ulnar Bowing Metrics and Distal Radioulnar Joint Metrics

		UV Correlation	P Value
Coronal: proximal bow	Bow depth	0.38	$P < .001$
	Proximal angle	0.39	$P < .001$
	Distal angle	0.23	$P < .001$
	Proximal angle to distal bow distal angle	–0.30	$P < .001$
Coronal: distal bow	Bow depth	–0.34	$P < .001$
	Proximal angle	–0.28	$P < .001$
	Distal angle	–0.48	$P < .001$
Sagittal bow	Bow depth	–0.17	$P < .001$
	Proximal angle	–0.15	$P < .001$
Sigmoid notch angle	Distal angle	–0.18	$P < .001$
		–0.77	$P = .01$

statistically significant differences between groups for the proximal angle ($P = .03$) and distal angle ($P = .01$) of the distal bow (Table 5).

Discussion

Managing DRUJ injuries often presents as a challenge, underscoring the need for a more comprehensive anatomical understanding. Our study leveraged 3D computer-aided design and segmentation software to explore the intricate relationships between ulnar bowing metrics and DRUJ landmarks. The main finding of our study was that intricate relationships exist between various ulnar bowing parameters and DRUJ landmarks.

We identified three distinct ulnar bows: one in the sagittal plane and two others—one proximal and one distal—in the coronal plane. These findings align with previous studies by Hreha et al and Weber et al, although our study provides a 3D approach. Hreha et al analyzed 98 plain radiographs to identify ulnar curvature, but measurements were limited by two-dimensional views. Weber et al used 422 cadaveric bone models to investigate ulnar morphology, but distal inspection at DRUJ was limited. Regardless, these studies identified sagittal bows of 6 mm and 5 mm in depth at 39% and 33% of the total length of the ulna for Hreha and Weber, respectively. Weber measured a proximal coronal bow of 10 mm in depth and 31.7% of the total length of the ulna. Hreha measured a distal coronal bow of 7 mm in depth and 75% of the total length of the ulna.^{14,16} All of these findings agree with our results reported here.

After establishing ulnar bowing metrics, we assessed relationships between full-length ulnar bowing and DRUJ morphology. Roner et al previously used 3D techniques to define local DRUJ morphology but did not relate these metrics to full ulnar bowing models. Notably, they identified sigmoid notch subtypes of positive, neutral, and negative SNA demonstrating inverse relationships to sigmoid notch radius and UV. Specifically, they found a moderate, negative correlation between SNA and UV; however, they did not correlate DRUJ metrics to full ulnar bowing models.¹⁵ We found similar intra-DRUJ measurements here, identifying the same

Table 4
Means and Correlations Between UV Subgroups and Distal Bow, Distal Angulation Metrics

UV Groups	Mean Distal Bow Angle	Distal Bow, Distal Angle Correlation
All UV	4.33	–0.48
Negative UV	5.20	–0.48
Neutral UV	4.79	–0.10
Positive UV	3.52	–0.27

sigmoid notch subtypes and a strong, negative correlation between the SNA and UV.

Ultimately, we discovered that various ulnar angulations and depths relate to the DRUJ. Our findings point to a 3D relationship impacting forearm rotation, where different angulations and depths of the ulna influence the DRUJ. The most salient finding was that distal ulnar bowing angulation moderately correlates with UV. This correlation has potential clinical relevance, particularly for procedures like ulnar shortening osteotomy, where precise UV adjustments significantly influence wrist stability and patient outcomes.

Summary and clinical implications

Ulnar impaction, DRUJ instability, and post-traumatic malrotation of the distal ulna are routinely treated with ligament stabilization, ulna shortening procedures, and more recently arthroplasty. Compared with other joints, the DRUJ has been less rigorously investigated. However, the DRUJ is anatomically complex with influences in 3D rotation with the radius and axial articulation with the ulnar-sided carpus. To date, surgical intervention with ulnar shortening osteotomy is frequently conducted to address these pathologies. This intervention only addresses anatomic correction in one plane and ignores any influence on the 3D articulation between the radius and ulna. This has been highlighted in previous investigations with the prevalence of reverse obliquity morphology at the DRUJ.² Authors have suggested caution in using ulnar

Table 5
Differences Between Groups for Dorsal or Volar Translations of the Ulnar Head*

Bow Type		Dorsal Translation Mean (n = 62)	Volar Translation Mean (n = 20)	P Value
Coronal: proximal bow	Bow depth	10.1	10.8	.31
	Proximal angle	2.1	2.0	.69
	Distal angle	3.9	3.9	.96
Coronal: distal bow	Bow depth	4.4	3.6	.07
	Proximal angle	2.1	1.7	.03*
	Distal angle	4.6	3.4	.01*
Sagittal bow	Bow depth	3.4	3.7	.52
	Proximal angle	1.9	2.2	.41
	Distal angle	2.0	1.8	.61

* Asterixed values represent statistical significance ($P < .05$).

shortening osteotomy in this morphology. Moreover, our study confirms that sagittal alignment and translation at the DRUJ articulation are directly related to ulna bowing at the distal ulna. This study clearly demonstrates these relationships in a precise 3D assessment to guide surgeons when planning correction of ulnar-sided pathology.

Limitations

Despite our comprehensive analysis, this study is not without limitations. Although we directly compared 3D reconstructions from 1 mm to 3 mm CT cuts for specific ulnar bowing landmarks, a similar comparison for specific DRUJ landmarks is lacking. Thus, we cannot conclusively affirm that 3 mm CT scans capture equivalent DRUJ detail. Software proficiency is another factor potentially affecting result reproducibility, although automation could mitigate this issue, particularly with machine learning algorithms incorporating tools such as curve feature identification or statistical shape models.^{18–22} Finally, the upper extremity scans used in this study were all considered “normal” and nonpathological, which could influence generalizability to “abnormal” variants.

Future directions

Our study enhances ulnar and DRUJ morphological comprehension by using 3D technology. The complex multiplanar curvature of the ulna necessitates a 3D approach for thorough understanding. Historically, surgeons have overlooked this multiplanar complexity during ulnar restoration, risking postoperative complications. Moving forward, incorporating distinct sagittal and coronal bowing patterns during surgical planning could optimize DRUJ alignment, improving postoperative outcomes. Future studies should investigate the impact of these parameters on patient-reported outcomes and expand to include cartilage modeling of the DRUJ and the radial morphology and its DRUJ relationship.

Conflicts of Interest

No benefits in any form have been received or will be received related directly to this article.

References

1. Thomas BP, Sreekanth R. Distal radioulnar joint injuries. *Indian J Orthop.* 2012;46(5):493–504.
2. O'Shaughnessy M, Shapiro LM, Schultz B, Retzky J, Finlay AK, Yao J. Morphology at the distal radioulnar joint: identifying the prevalence of reverse obliquity. *J Wrist Surg.* 2020;9(5):417–424.
3. Haugstvedt JR, Langer MF, Berger RA. Distal radioulnar joint: functional anatomy, including pathomechanics. *J Hand Surg Eur Vol.* 2017;42(4):338–345.
4. Small RF, Taqi M, Yaish AM. Radius and ulnar shaft fractures. In: *StatPearls*. StatPearls Publishing; 2023. Accessed July 16, 2023. <http://www.ncbi.nlm.nih.gov/books/NBK557681/>
5. Morway GR, Miller A. Clinical and radiographic evaluation of ulnar-sided wrist pain. *Curr Rev Musculoskelet Med.* 2022;15(6):590–596.
6. Bain GI, Pourgiezis N, Roth JH. Surgical approaches to the distal radioulnar joint. *Tech Hand Up Extrem Surg.* 2007;11(1):51–56.
7. Atzei A, Rizzo A, Luchetti R, Fairplay T. Arthroscopic foveal repair of triangular fibrocartilage complex peripheral lesion with distal radioulnar joint instability. *Tech Hand Up Extrem Surg.* 2008;12(4):226–235.
8. Iniesta A, Bonev B, Curvale C, Legré R, Gay A. Outcomes of ulnar shortening osteotomy using a new compression plate. *Hand Surg Rehabil.* 2020;39(1):19–22.
9. Poppler LH, Moran SL. Acute distal radioulnar joint instability: evaluation and treatment. *Hand Clin.* 2020;36(4):429–441.
10. Boyd B, Adams J. Distal radioulnar joint instability. *Hand Clin.* 2021;37(4):563–573.
11. Chan SKL, Singh T, Pinder R, Tan S, Craigen MA. Ulnar shortening osteotomy: are complications under reported? *J Hand Microsurg.* 2015;7(2):276–282.
12. Barbaric K, Rujevcan G, Labas M, Delimar D, Bicanic G. Ulnar shortening osteotomy after distal radius fracture malunion: review of literature. *Open Orthop J.* 2015;9:98–106.
13. Darlis NA, Ferraz IC, Kaufmann RW, Sotereanos DG. Step-cut distal ulnar-shortening osteotomy. *J Hand Surg.* 2005;30(5):943–948.
14. Hreha J, Congiusta DV, Ahmed IH, Vosbikian MM. What is the normal ulnar bow in adult patients? *Clin Orthop.* 2020;478(1):136–141.
15. Roner S, Fürnstahl P, Scheibler AG, Sutter R, Nagy L, Carrillo F. Three-dimensional automated assessment of the distal radioulnar joint morphology according to sigmoid notch surface orientation. *J Hand Surg.* 2020;45(11):1083.e1–1083.e11.
16. Weber MB, Olgun ZD, Boden KA, et al. A cadaveric study of radial and ulnar bowing in the sagittal and coronal planes. *J Shoulder Elbow Surg.* 2020;29(5):1010–1018.
17. Yong WJ, Tan J, Adikrishna A, et al. Morphometric analysis of the proximal ulna using three-dimensional computed tomography and computer-aided design: varus, dorsal, and torsion angulation. *Surg Radiol Anat SRA.* 2014;36(8):763–768.
18. Mauler F, Langguth C, Schweizer A, et al. Prediction of normal bone anatomy for the planning of corrective osteotomies of malunited forearm bones using a three-dimensional statistical shape model. *J Orthop Res Off Publ Orthop Res Soc.* 2017;35(12):2630–2636.
19. Vlachopoulos L, Székely G, Gerber C, Fürnstahl P. A scale-space curvature matching algorithm for the reconstruction of complex proximal humeral fractures. *Med Image Anal.* 2018;43:142–156.
20. Rodriguez-Florez N, Bruse JL, Borghi A, et al. Statistical shape modelling to aid surgical planning: associations between surgical parameters and head shapes following spring-assisted cranioplasty. *Int J Comput Assist Radiol Surg.* 2017;12(10):1739–1749.
21. Horbaly H, Hubbe M, Sylvester AD, Steadman DW, Auerbach BM. Variation in human limb joint articular morphology. *Am J Biol Anthropol.* 2023;182(3):388–400.
22. Zhao W, Guo Y, Xu C, et al. Distal humerus morphological analysis of chinese individuals: a statistical shape modeling approach. *Orthop Surg.* 2022;14(10):2730.